Journal of the Mechanics and Physics of Solids 84 (2015) 196–213

Contents lists available at ScienceDirect

Journal of the Mechanics and Physics of Solids

journal homepage: www.elsevier.com/locate/jmps

Exploring the relationship between critical state and particle shape for granular materials

J. Yang [a,*], X.D. Luo [a]

[a] Department of Civil Engineering, The University of Hong Kong, Hong Kong, China

ARTICLE INFO

Article history:
Received 5 March 2015
Received in revised form
3 August 2015
Accepted 3 August 2015
Available online 4 August 2015

Keywords:
Constitutive relations
Critical state theory
Granular material
Particle shape
Shear behavior

ABSTRACT

The relationship between critical state and particle shape corresponds to the most fundamental aspect of the mechanics of granular materials. This paper presents an investigation into this relationship through macro-scale and micro-scale laboratory experiments in conjunction with interpretation and analysis in the framework of critical state soil mechanics. Spherical glass beads and crushed angular glass beads of different percentages were mixed with a uniform quartz sand (Fujian sand) to create a sequence of mixtures with varying particle shape. On the micro-scale, particle shape was accurately measured using a laser scanning technique, and was characterized by aspect ratio, sphericity and convexity; a new shape index, taken as the average of the three shape measures and referred to as overall regularity, was proposed to provide a collective characterization of particle shape. On the macro-scale, both undrained and drained triaxial tests were carried out to provide evidence that varying particle shape can alter the overall response as well as the critical states in both stress space and volumetric compression space. The mixtures of Fujian sand and spherical glass beads were found to be markedly more susceptible to liquefaction than the mixtures of Fujian sand and crushed angular glass beads. The change in liquefaction susceptibility was shown to be consistent with the change in the position of the critical state locus (CSL) in the compression space, manifested by a decrease in the intercept and gradient of the CSL due to the presence of spherical glass beads. Quantitative relationships have been established between each of the critical state parameters and each of the shape parameters, thereby providing a way to construct macro-scale constitutive models with intrinsic micro-scale properties built in.

1. Introduction

Granular materials refer to a class of natural and synthetic materials consisting of individual particles that interact with each other when subjected to loading. These materials behave differently from usual solids and exhibit many salient features such as dilatancy, anisotropy, pressure dependence, density dependence, and nonlinear elasticity. The mechanical behavior of granular materials is a subject of long-standing interest in many fields, with both scientific fascination and practical importance (Spencer, 1964; Rudnicki and Rice, 1975; Satake and Jenkins, 1988; Nedderman, 1992; Jaeger et al., 1996; McDowell et al., 1996; Collins and Houlsby, 1997; Nixon and Chandler, 1999; Anand and Gu, 2000; Rothenburg and Kruyt, 2004; Gu and Yang, 2013; Andreotti et al., 2013; Goddard, 2014; Li and Dafalias, 2015; and the references therein). For

* Corresponding author. Fax: +852 2559 5337.
E-mail address: junyang@hku.hk (J. Yang).

http://dx.doi.org/10.1016/j.jmps.2015.08.001
0022-5096/

Nomenclature

AR	aspect ratio
C	convexity
C_u	coefficient of uniformity
CSL	critical state locus
D^{Fmax}	maximum Feret diameter
D^{Fmin}	minimum Feret diameter
e	void ratio (ratio of the volume of voids to the total volume of the soil or the packing)
e_Γ	void ratio intercept (for the CSL in the power-law form)
M	effective stress ratio at the critical state
OR	overall regularity
p	hydrostatic stress or mean effective stress in triaxial test ($=(\sigma_1+2\sigma_3)/3$)
q	deviatoric stress in triaxial test ($=\sigma_1-\sigma_3$)
R	roundness
S	sphericity
ε_a	axial strain in triaxial test
ε_v	volumetric strain
ϕ_{cs}	critical state friction angle
Γ	void ratio intercept (for CSL in the semi-log form)
λ	slope of the CSL in the e–log p plane
λ_c	slope of the CSL in the e–p plane with the power-law form
σ_1, σ_3	major and minor principal stress
$\boldsymbol{\sigma}$, $\mathbf{s}$	stress tensor and deviatoric stress tensor
$\boldsymbol{\varepsilon}$, $\boldsymbol{\varepsilon}_d$	strain tensor and deviatoric strain tensor
$\mathbf{I}$	identity tensor

many geotechnical engineering applications, properly predicting the behavior of granular soils under undrained (i.e. constant volume) and drained conditions plays a crucial role, yet remains an area of considerable uncertainty and difficulty. The complexity originates mainly from the particulate nature of soils: that is, a granular soil can exist over a range of densities at constant stress and the spectrum of states corresponds to a variety of responses ranging from flow liquefaction to strain hardening. From the perspective of micromechanics, the overall response of a granular soil is highly dependent on the packing patterns and interactions of the constituent particles which are, further, closely related to the characteristics of the particles. The key particle characteristics for coarse grained soils include particle size, particle size distribution, particle shape and mineralogy. Research interest has been growing in the influence of particle characteristics on the behavior of granular soils, resulting in valuable data and insights that contribute to an improved understanding in several aspects (e.g., Sukumaran and Ashmawy, 2001; Cho et al., 2006; Rouse et al., 2008; Wichtmann and Triantafyllidis, 2009; Cavarretta et al., 2010; Yang and Wei, 2012; and the references therein).

Among the various grain characteristics, particle size and gradation can routinely be determined using sieve analysis in soil mechanics laboratories and their influence has received relatively more attention. In contrast, less discussion exists on quantifying the role of particle shape in the overall response of granular soils, due probably to the difficulty involved in grain-scale measurement. In most geotechnical engineering practice and research, accurate measurement of particle shape is not required on a routine basis and the information on particle shape is usually provided in qualitative terms for a given soil. If a quantitative shape analysis is made, the common approach is to make use of the chart proposed by Krumbein and Sloss (1963), as for example in the study of Cho et al. (2006). The chart is arranged as a 4×5 matrix of 2D images of reference particles, in which each row includes five particles with the same sphericity but different values of roundness and each column includes four particles with the same roundness but different values of sphericity. The roundness and sphericity of a given particle are assessed by visual comparison with the reference shapes in the chart. The method is time consuming and not feasible for assessing large numbers of particles, and because of the subjective nature the level of accuracy may not be high. To improve accuracy, one can choose to calculate the roundness of a particle directly from the measurements on the particle image by using the Wadell (1932) method (e.g., Rouse et al., 2008) or by use of complex Fourier analysis (Bowman et al., 2001). Nevertheless, the direct measurement remains tedious and is viable only for a small number of particles. More efficient and reliable methods for grain shape analysis are needed. On the macro-scale, various aspects of granular soil behavior, particularly the density and pressure dependences, have been successfully characterized and modeled in the theoretical framework known as critical state soil mechanics (CSSM). The kernel of the framework is the existence of an ultimate state of shear failure (Schofield and Wroth, 1968; Poulos, 1981; Been and Jefferies, 1985; Wood, 1990), termed as critical state or steady state, at which the soil deforms continuously under constant stress and constant volume. Analytically this state can be described as

$$\begin{cases} \dot{p} = 0 \\ \dot{\mathbf{s}} = \mathbf{0} \\ \dot{\varepsilon}_v = 0 \\ \dot{\boldsymbol{\varepsilon}}_d \neq \mathbf{0} \end{cases} \tag{1}$$

where p is the hydrostatic stress, defined in terms of the stress tensor $\boldsymbol{\sigma}$ as $p = (1/3)\mathrm{tr}\boldsymbol{\sigma}$; $\mathbf{s} = \boldsymbol{\sigma} - p\mathbf{I}$ is the deviatoric part of the stress tensor; ε_v is the volumetric strain, defined in terms of the strain tensor $\boldsymbol{\varepsilon}$ as $\varepsilon_v = \mathrm{tr}\boldsymbol{\varepsilon}$; $\boldsymbol{\varepsilon}_d = \boldsymbol{\varepsilon} - (\varepsilon_v/3)\mathbf{I}$is the deviatoric part of the strain tensor; the superposed dot denotes the rate or an increment of the quantity. Note that as usual in soil mechanics, both stress and strain quantities are assumed positive in compression and all stress components throughout this paper are considered effective (that is, $\boldsymbol{\sigma} = \bar{\boldsymbol{\sigma}} - u\mathbf{I}$, with $\bar{\boldsymbol{\sigma}}$ being the total stress tensor and u the pore water pressure).

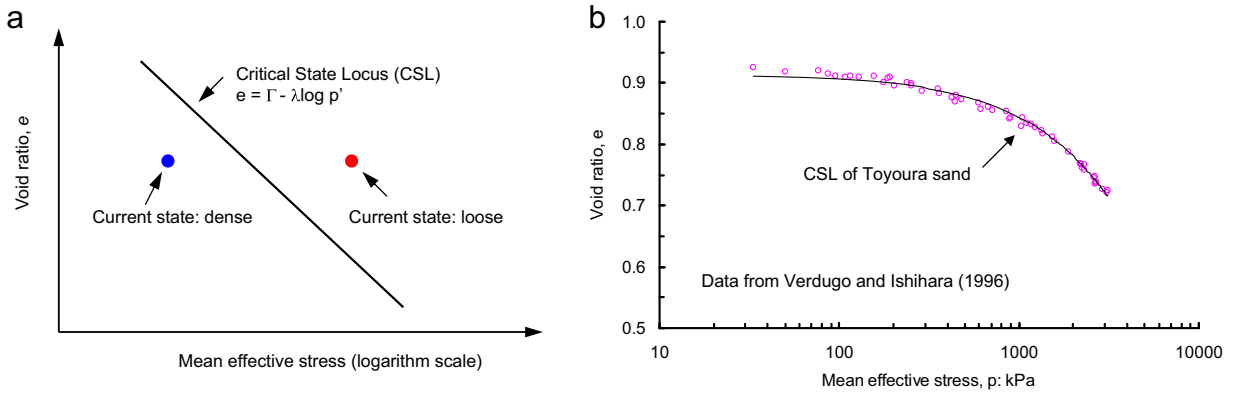

Fig. 1. Representation of critical states: (a) in e–log p' plane as a straight line; (b) in e–log p′ plane as a curved line.

In drained or undrained triaxial tests in soil mechanics, critical states are attained at large strains with an effective stress ratio M, constituting a straight line in the stress space as follows:

$$q = Mp \tag{2}$$

where $q = \sqrt{(3/2)\mathbf{s}:\mathbf{s}} = (\sigma_1 - \sigma_3)$ is the deviatoric stress and $p = (\sigma_1 + 2\sigma_3)/3$ is the mean effective stress in standard triaxial notations, with σ_1 and σ_3 $(=\sigma_2)$ as the principal stress. In the compression space, the locus of critical states is often represented by a linear function as follows (Fig. 1a):

$$e = e_c = \Gamma - \lambda \log p \tag{3}$$

where e is the void ratio, defined as the ratio of the volume of voids to the total volume of the soil element; e_c denotes the void ratio of the soil at critical state; λ is the slope of the straight line; and Γ is the void ratio intercept, typically taken at $p=1$ kPa.

Eqs. (2) and (3) provide a complete specification of the critical state locus (CSL) for a given soil, and the three parameters M, Γ and λ form a set of basic parameters that are needed in CSSM-based constitutive models (e.g., Wood, 1990; Gajo et al., 2004). Whilst Eq. (3) offers a simple representation of the CSL in the compression space, there is increasing evidence (e.g., Verdugo and Ishihara, 1996; Yang and Wei, 2012) that the CSL is a curved rather than straight line on the semi-log scale, as given in Figs.1b and 2a using experimental data on Toyoura sand and Fujian sand. Caution should therefore be exerted about inaccuracies of the linear function in representing the critical states and the consequences for predicting the mechanical response – this is because the CSL in the critical state framework serves as a reference state separating the initial soil states into contractive and dilative regions. In this regard, a more accurate and reasonable representation of the CSL is needed, and this can be achieved by using a power law function as follows (Li and Wang, 1998):

$$e = e_c = e_\Gamma - \lambda_c \left(\frac{p}{p_a}\right)^n \tag{4}$$

where e_Γ is the void ratio intercept at $p=0$, and λ_c relates to the slope of the straight line (Fig. 2b). For a range of sands and sand-fines mixtures, the exponent n has been found to take an optimal value of 0.6 (Yang and Wei, 2012). The above

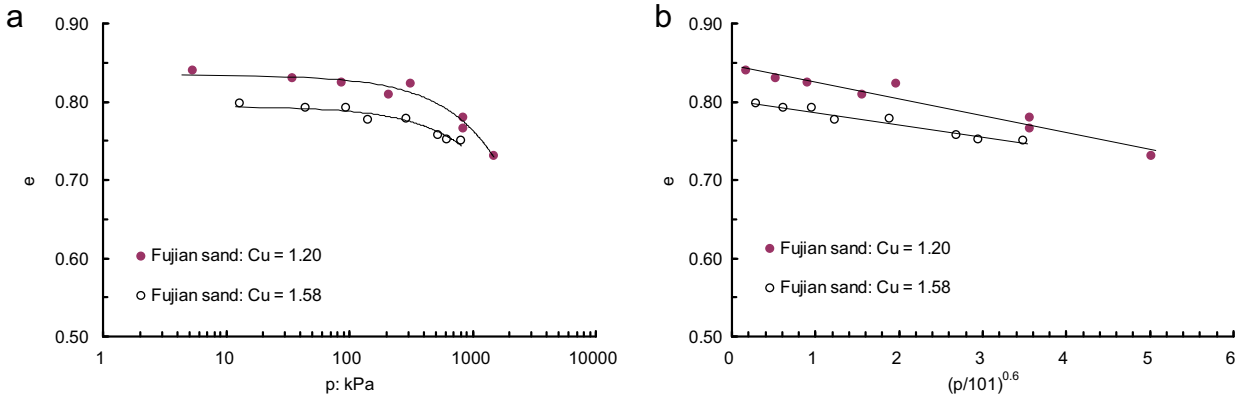

Fig. 2. Influence of particle grading on the position of critical state locus in e–p′ plane: (a) semi-log form and (b) power-law form.

expression has been adopted in many recent constitutive models to better represent the CSL and predict the response of granular soils (e.g., Taiebat and Dafalias, 2008).

Within the CSSM framework the parameters M, e_Γ, and λ_c should be regarded as intrinsic properties that do not vary with the state or the boundary conditions under which a soil exists. Their values are expected to reflect the nature of the constituent particles, such as grading and shape. Here arise two important questions that relate to the most fundamental aspect of the mechanics of granular soils: (a) *are there any relationships between these macro-scale intrinsic properties and those at the micro (grain) scale*, and (b) *if yes, how are they related?* This paper presents a study that attempts to address these two questions through a specifically designed experimental program, with focus on exploring the relationship between the critical state properties (M, e_Γ, λ_c) and particle shape parameters.

In so doing, an experimental program including laboratory tests at both macro and micro-scales has been carefully designed with several key considerations. First, test materials should be controlled so that they possess similar grading but distinct particle shapes – this is to isolate the influence of grading from that of particle shape. In several previous studies on the influence of particle shape, notable differences existed in the coefficient of uniformity (C_u) of the test materials and thus it is difficult to distinguish the influence of particle shape from the potential influence of grading. In other words, the observed differences in overall response in those tests cannot be simply attributed to the influence of particle shape because the differences in grading may play a role as well.

To make the above point clear, a Fujian sand, which has a larger C_u value than the standard Fujian sand tested by Yang and Wei (2012), was sieved in the laboratory to produce two samples with different gradings: $C_u = 1.20$ and 1.58, respectively. For each sample of the sand, a series of triaxial tests was performed to determine its critical states in the compression space as shown in Fig. 2, where the semi-log form is given in Fig. 2a and the power-law form is given in Fig. 2b. One can see that even a small difference in C_u results in an appreciable change in the position of the CSL (particularly in the void ratio intercept).

The second consideration is that particle shape should be quantified using objective and accurate measurements and, for a given particle, multiple shape parameters should be used. Each shape parameter needs to be determined with a sample of measurements large enough so that the representative value obtained becomes insensitive to additional measurements. This consideration is to ensure that for a given granular material, the shape of its constituent particles can be characterized in a more reliable and comprehensive way. Additionally, the particle shape of test materials needs to be systematically varied so that quantitative relations between shape parameters and critical state properties for these materials may be discovered.

This paper presents the main results from this specifically designed experimental program along with a detailed interpretation and analysis. An emphasis of the paper is on quantifying the influence of particle shape in the CSSM framework and at the same time providing unique datasets that can serve as a useful reference for validation and calibration of

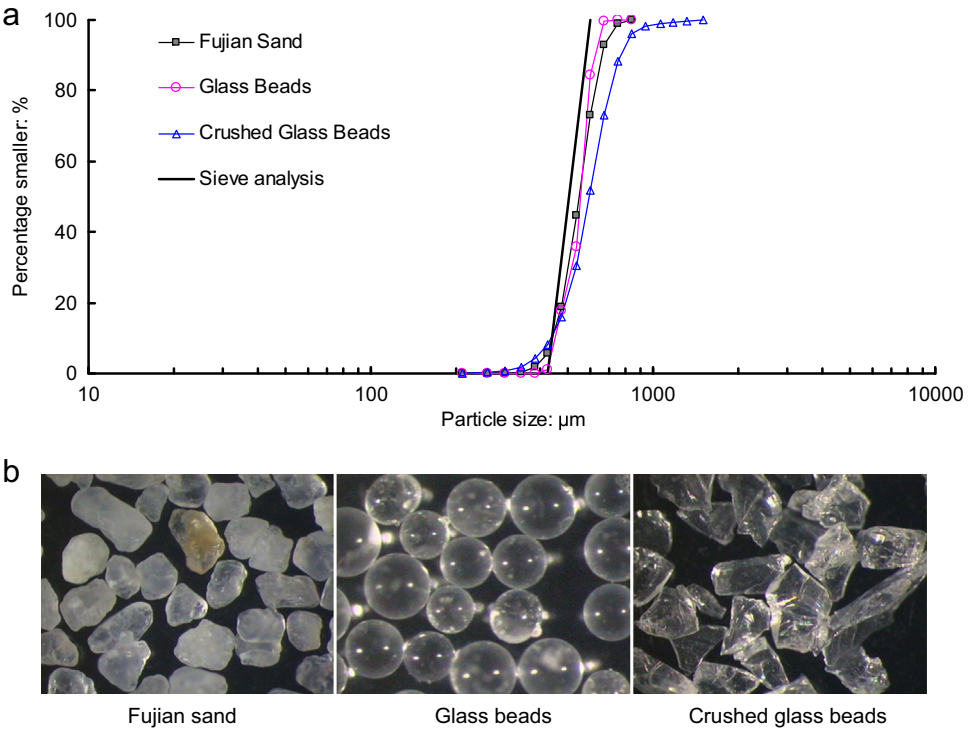

Fig. 3. Test materials of sand size: (a) particle size distribution curves; (b) microscope photographs.

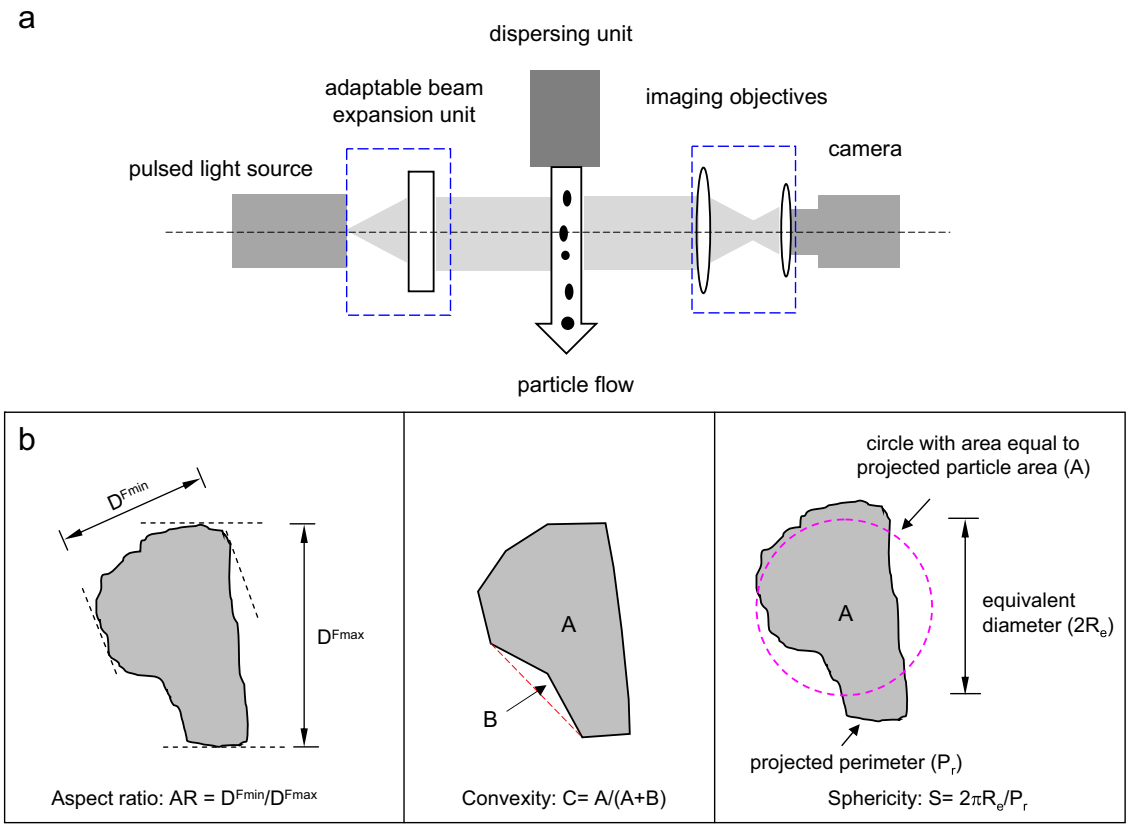

Fig. 4. Schematic illustration of particle characterization technique: (a) QICPIC apparatus (redrawn after Sympatec 2008); (b) definitions for particle size and shape.

constitutive models and discrete element simulations for granular materials.

2. Test materials and particle characteristics

The experiments involved three base materials of similar grading but distinct particle shape: the medium quartz Fujian sand with sub-rounded grains, the as-supplied spherical glass beads and the crushed angular glass beads.

2.1. Particle size and grading

The particle size distribution curves of the three materials were controlled by sieving to be exactly the same (Fig. 3a), giving the mean size of 512.5 μm and the C_u of 1.2. The microscopy photographs of these materials are shown in Fig. 3b. Adding to the conventional sieve analysis, an imaging-based method was also used to determine particle size and grading for these materials. The results are also included in Fig. 3a for the purpose of comparison. The principle of the imaging-based method is similar to the method described in Yang and Wei (2012), but the apparatus is more robust and versatile. The apparatus (known as QICPIC) comprises several key elements as sketched in Fig. 4a; the general testing procedure involves feeding a sample of particles into the feeding unit to generate a steady particle flow through the vertical shaft, which is then captured by the specially configured light source and imaging lenses and recorded by the camera in the form of a sequence of binary images. The apparatus incorporates several measures, such as controlled vibration and vacuum extraction, to minimize the tendency for preferred alignments of the particles during the flow process, thereby providing more realistic measurements of the images than the conventional optical analysis. The apparatus has been successfully used in recent years to characterize soil particle shape (e.g., Cavarretta, 2009; Altuhafi et al., 2013). A detailed description of how the apparatus works is beyond the scope of this paper but can be found in Sympatec (2008).

For a given particle, several size measures can be derived from the imaging-based system, for example the maximum Feret diameter (D^{Fmax}), the minimum Feret diameter (D^{Fmin}) and the mean Feret diameter. As illustrated in Fig. 4b, the Feret diameter is defined as the distance between two tangents on opposite sides of the particle. For each of the three materials the use of D^{Fmin} as the size index has been found to consistently provide the grading curve that is close to that determined by sieve analysis (Fig. 3a). This finding is consistent with that of Altuhafi et al. (2013) on Toyoura sand. Also, an interesting

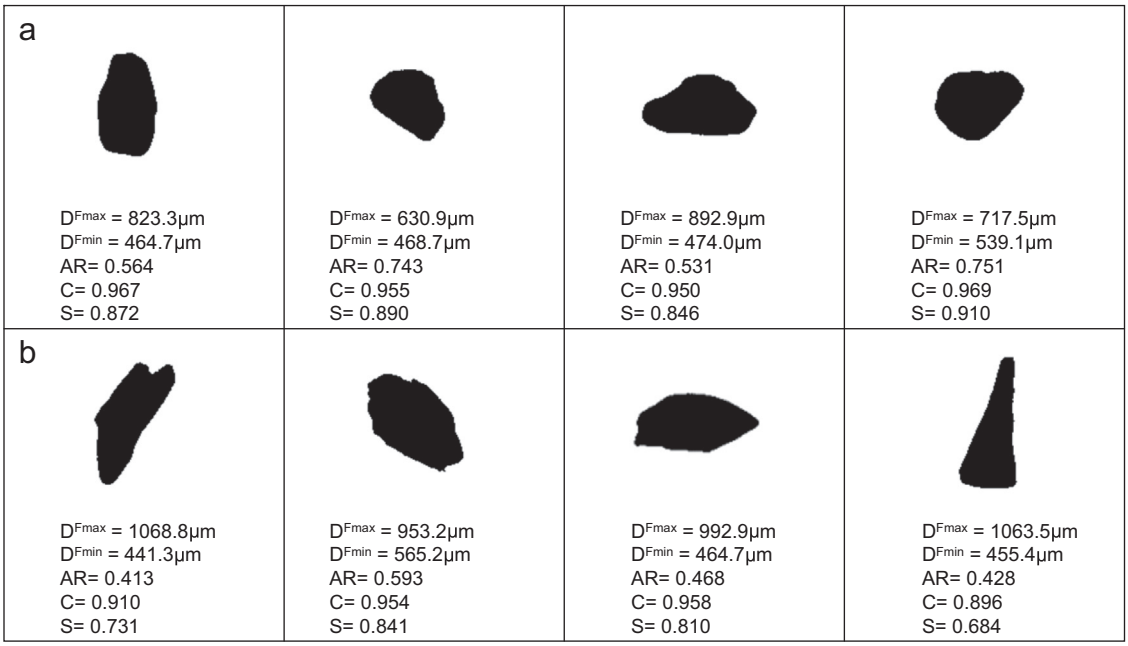

Fig. 5. Binary images and shape parameters of representative particles: (a) Fujian sand; (b) crushed glass beads.

observed feature is that the grading curve determined by this new technique for glass beads correlates best with that derived from sieve analysis, whereas the grading curve for crushed glass beads deviates most from the sieve data. This observation suggests that particle shape has an influence on particle size measurements when using the imaging-based method. A similar observation was obtained by Yang and Wei (2012) in measuring particle sizes for sand-sized and silt-sized

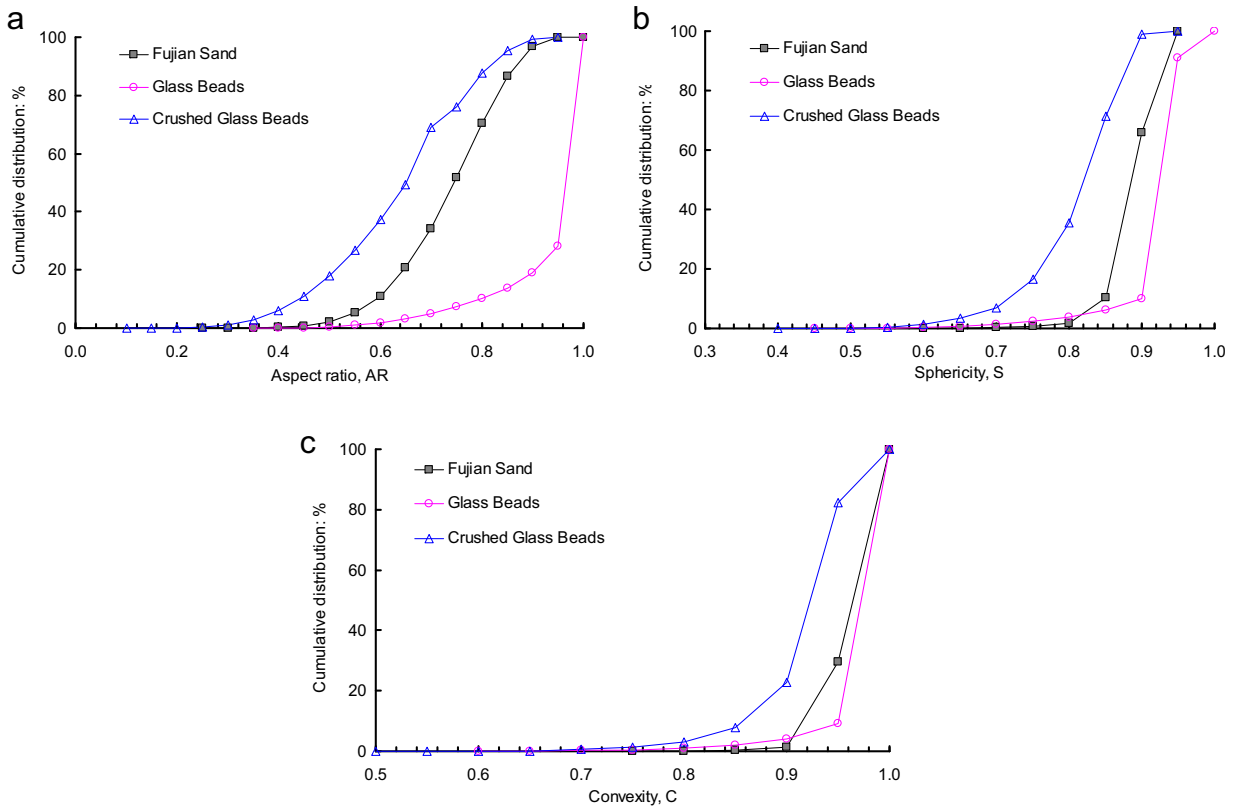

Fig. 6. Cumulative distribution curves of shape parameters: (a) aspect ratio; (b) sphericity; (c) convexity.

materials.

2.2. Particle shape measurements

Of particular interest here is to make objective and accurate measurements of particle shape. For a given particle, three shape measures can be made using the apparatus, namely the aspect ratio (AR), the convexity (C) and the sphericity (S). Referring to Fig. 4b, the aspect ratio is defined as the ratio between D^{Fmin} and D^{Fmax}; the convexity is the area of the particle (A) divided by its area if any concavities within its perimeter are filled ($A+B$); the sphericity is defined as the ratio of the perimeter of a circle with the same area as the projected area of the particle to its actual perimeter. As noted by Cavarretta et al. (2010), the sphericity given in the reference chart of Krumbein and Sloss (1963) was essentially based on aspect ratio and thus it differs from the sphericity defined here. Also, it should be noted that the sphericity is defined for 2D images and hence differs from that defined for 3D images (Fonseca et al., 2012); for the former the measured values are between 0 and 1, with the upper limit for an ideally spherical shape, whereas for the latter the measured values can be greater than 1 and this is somehow odd. A detailed discussion of the differences between the two measurements of sphericity is outside the scope of this study; readers may refer to Alshibi et al. (2014) and Fonseca et al. (2012) for relevant details.

As an example, Fig. 5a presents the shape and size data for several selected Fujian sand grains along with the binary images captured by the apparatus, while Fig. 5b gives the binary images of representative crushed glass beads and their shape and size data. By comparison, the crushed glass beads have generally smaller values of AR, S and C, meaning that they are more angular and irregular than Fujian sand grains. This is consistent with the qualitative observation on the microscopy images in Fig. 3b. For each of the shape measures, a general trend can be observed that as the shape value increases, the geometry of the particle tends to be more rounded and regular. In this respect, a new shape measure, referred to as overall regularity (OR) and defined as the average of the three shape measures, is proposed as follows to characterize particle shape in a collective manner:

$$OR = (AR + S + C)/3 \tag{5}$$

Note that the above shape descriptor differs from the regularity of Cho et al. (2006), which was defined as the average of Krumbein and Sloss's sphericity and roundness.

To obtain representative and repeatable shape data for each material, the cumulative distribution curves of AR, S and C were established from a large sample of the material (about 30 g with tens of thousands of grains), as shown in Fig. 6. An interesting feature of these curves is that for any shape parameter (AR, S or C), the crushed angular glass beads always exhibit the broadest distribution whereas the spherical glass beads always show the narrowest distribution, with the distribution curve of Fujian sand in between the two. For a given material it is reasonable to choose the shape value corresponding to the 50% cumulative distribution as a representative value: for example the representative AR values for Fujian sand, glass beads and crushed glass beads were determined to be 0.745, 0.974 and 0.653, respectively, and the representative sphericity (S) values for the three materials were determined as 0.891, 0.944 and 0.822. For clarity the size and shape data for the three materials are summarized in Tables 1 and 2.

To investigate systematically the behavior of granular materials with varying particle shape, the spherical glass beads and crushed angular glass beads of different percentages were mixed with Fujian sand to produce a sequence of binary mixtures, including 80% sand–20% glass beads (denoted as FS80G20), 60% sand–40% glass beads (FS60G40), 80% sand–20% crushed glass beads (FS80C20), and 60% sand–40% crushed glass beads (FS60C40). For these binary mixtures, the concept of combined roundness (Yang and Wei, 2012) was generalized to define a set of combined shape parameters, each of them depending on the corresponding shape values of the component materials and their percentages. For example, the combined AR value for mixture FS80G20 is determined by

$$AR_{\_FS80G20} = AR_{\_Fujiansand} \times 80\% + AR_{\_glassbeads} \times 20\% \tag{6}$$

The above expression gives an AR value of 0.791 for the mixture, which is reasonable in comparison with 0.745 for pure Fujian sand and 0.974 for glass beads. For ease of reference, all shape data for the mixtures in the study are summarized in Table 2.

Table 1
Particle size data for base materials.

Material	Sieve analysis (size in μm)				QICPIC analysis (size in μm)			
	D_{10}	D_{50}	D_{60}	C_u	D_{10}	D_{50}	D_{60}	C_u
Fujian sand	442.5	512.5	530.0	1.2	441.9	547.1	570.0	1.29
Glass beads	442.5	512.5	530.0	1.2	451.6	554.0	567.3	1.26
Crushed glass beads	442.5	512.5	530.0	1.2	436.8	594.4	627.2	1.44

Note: D_{10}=largest particle size in the smallest 10% of particles; D_{50}=mean particle size;
D_{60}=largest particle size in the smallest 60% of particles; C_u=coefficient of uniformity=D_{60}/D_{10}

Table 2
Measured data on particle shape.

Material	Aspect ratio (AR)	Sphericity (S)	Convexity (C)	Overall regularity (OR)	Roundness (R)
Fujian sand	0.745	0.891	0.956	0.864	0.470
Glass beads	0.974	0.944	0.974	0.964	1.000
Crushed glass beads	0.653	0.822	0.929	0.801	0.390
Mixture FS80G20	0.791	0.901	0.960	0.884	0.576
Mixture FS60G40	0.837	0.912	0.963	0.904	0.682
Mixture FS80C20	0.727	0.877	0.951	0.852	0.454
Mixture FS60C40	0.708	0.863	0.945	0.839	0.438

3. Overall macro-scale behavior

To provide a comprehensive assessment of how overall behavior is altered by varying particle shape, both drained and undrained triaxial tests were carried out on pure sand and binary mixtures by using an automatic computer-controlled triaxial apparatus. All specimens, each 71.1 mm in diameter and 142.2 mm in height, were prepared by the moist tamping method with the under-compaction technique (Ladd, 1974). This method was chosen because it can produce a range of soil densities and has the advantage of preventing grain segregation and yielding uniform specimens. All specimens were saturated in two stages: initially by flushing the specimen with carbon dioxide and de-aired water, and then by applying back pressure. Specimens with the Skempton B-value (Ladd, 1974) greater than 0.95 were considered saturated. After saturation, each specimen was isotropically consolidated to the target mean effective stress, from which compression was started with a specified small strain rate.

Typical results from a series of drained tests on Fujian sand and its mixtures with glass beads (FS80G20 and FS60G40) are shown in Fig. 7a. For all three specimens, the initial effective confining stress was set at 500 kPa and the post-consolidation void ratio was around 0.820. While the pattern of stress–strain curve remained similar, adding glass beads into Fujian sand was found to decrease the shear strength, and as the percentage of glass beads increased the strength reduction became more remarkable. Interestingly, a completely reversed tendency was obtained for mixtures of Fujian sand and crushed glass beads (FS80C20 and FS60C40) when subjected to the same testing conditions, as shown in Fig. 7b. Given shape data for

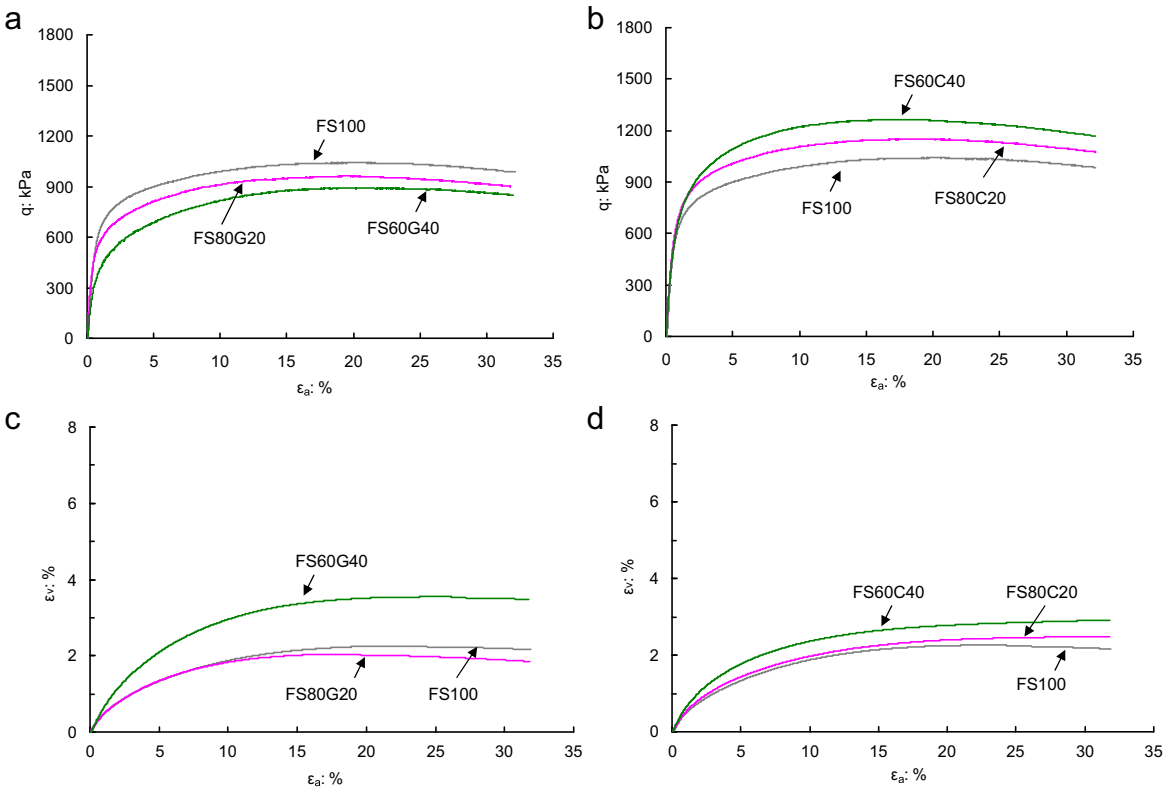

Fig. 7. Drained shear behavior ($p'=500$ kPa, $e=0.820$): (a) and (c) Fujian sand mixed with glass beads; (b) and (d) Fujian sand mixed with crushed glass beads.

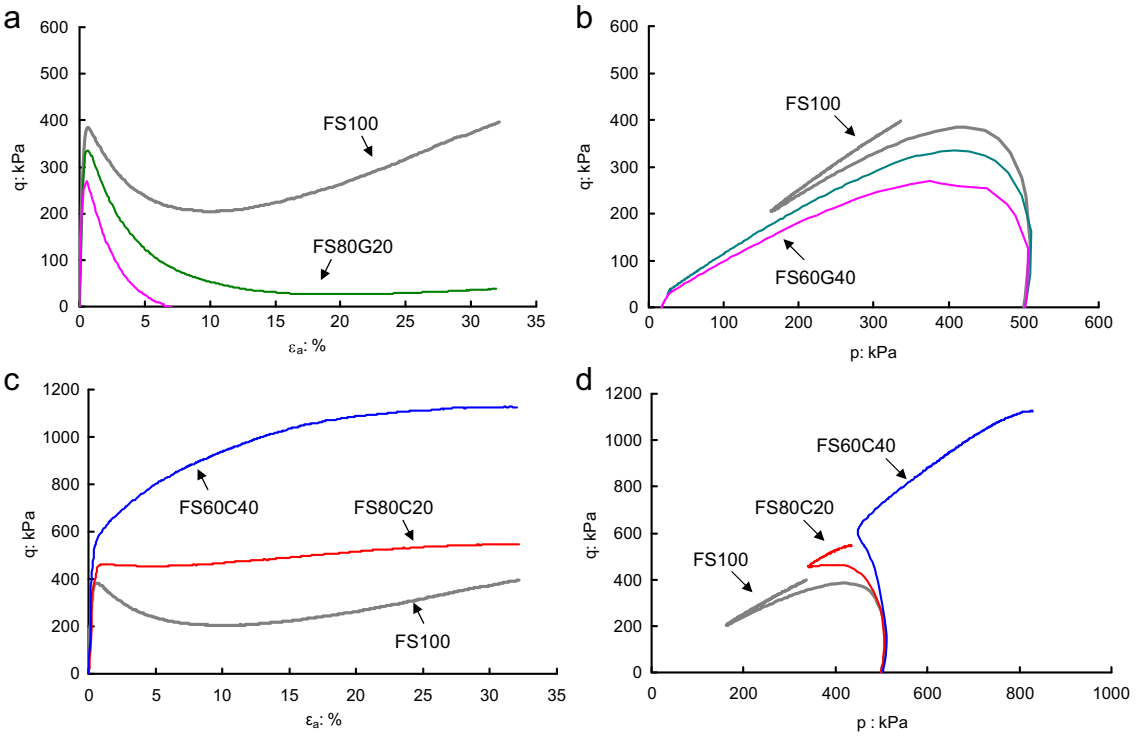

Fig. 8. Undrained shear behavior ($p'=500$ kPa, $e=0.820$): (a) and (b) Fujian sand mixed with glass beads; (c) and (d) Fujian sand mixed with crushed glass beads.

these materials (Table 2), one can infer that, other things being equal, granular materials with regular and rotund particles tend to have lower drained shear strength than those with irregular and angular particles.

The stress–strain curves (Fig. 7a and b) and the volumetric strain response (Fig. 7c and d) from the drained tests indicate that each specimen tended towards a critical state at the end of shearing. Indeed, the rate of variation of the deviatoric stress or the volumetric strain at strains of 25–30% was found to be rather small; from any practical point of view the state at this strain level can be considered to be associated with the critical state. A similar consideration was used by Verdugo and Ishihara (1996) to define critical states for Toyoura sand from their triaxial tests.

For the same initial state ($p=500$ kPa and $e=0.820$), a series of undrained triaxial tests was also conducted on Fujian sand and the four mixtures. The change in the behavioral pattern associated with varying particle shape is immediately evident in Fig. 8. As seen in Fig. 8a and b, the addition of glass beads into Fujian sand was found to always cause an increase in strain softening as compared with the sand on its own at a similar void ratio. As the quantity of glass beads increased, the mixed sand sample tended to become more contractive and liquefiable. Mixture FS60G40 shows an almost ideal liquefaction

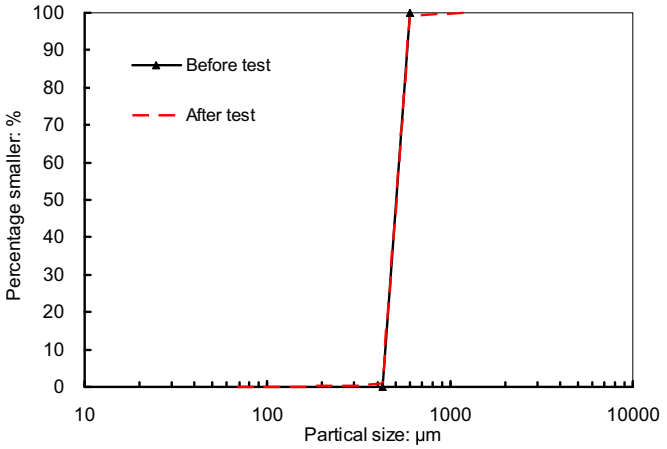

Fig. 9. Particle size distribution curves of mixed sand sample FS80G20 before and after testing.

behavior, with a complete loss of the strength at the end of shearing, whereas the pure sand sample exhibits a typical transitional behavior, characterized by a limited loss of strength (or limited liquefaction) and the occurrence of the so-called quasi-steady state (Verdugo and Ishihara, 1996). From the perspective of micromechanics, this quasi-steady state is associated with the most pronounced loss of contacts during shearing (Yang and Dai, 2011).

A reversed tendency was observed in mixtures of Fujian sand and crushed glass beads, as shown in Fig. 8c and d. Adding crushed glass beads into Fujian sand always led to a decrease of strain softening and as the proportion of crushed glass beads increased, the mixture became more dilative. While pure Fujian sand exhibited the transitional response with limited liquefaction, the overall response of the mixture FS60C40 was highly strain hardening, without any signs of liquefaction or strength loss. The deviatoric stress achieved by the mixed sample at large strains was almost three times that attained by the pure sand sample. Although the behavioral patterns appeared to be very diverse, all specimens were brought towards the critical state at the end of undrained shearing, with almost constant shear stresses at the large strain level.

In all tests no visible strain localization was observed. The possibility of particle breakage was also checked by comparing particle size distribution curves before and after the tests (an example is shown in Fig. 9 for mixture FS80G20), and no significant breakage was found in these tests. This is not a surprising observation, because the stresses involved in the experiments (<2 MPa) are much lower than the stress level that can cause significant breakage of quartz sand grains and glass beads. Verdugo and Ishihara (1996) conducted triaxial tests on Toyoura sand and reported no particle breakage within the stress level applied (<4 MPa). For glass beads, the stress level for the occurrence of significant breakage is expected to be over 10 MPa, which is far beyond the stress range of most practical interest. An important notion in this respect is that the curvature of the CSL in the e–$\log p$ plane is *not necessarily attributed to particle breakage*.

4. Representation of critical states

A more detailed examination is needed of how the critical states attained in these tests are represented in the stress space and in the volumetric compression space and whether varying particle shape can impose a notable influence on such representations. This is a necessary step before any shape effect on the critical state properties can be quantified.

4.1. Critical state locus in the q–p plane

The critical states attained by Fujian sand in both undrained (CU) and drained (CD) tests in the q–p plane are shown in Fig. 10. These data points can perfectly be fitted by a single line passing though the origin (with $R^2=1$), providing excellent evidence that the critical state locus is independent of drainage conditions. The slope of the straight line (i.e. M) is quantified to be 1.21. Furthermore, the critical state data for four binary mixtures are plotted in Fig. 11. For each mixture, both undrained and drained test data are fitted perfectly by a straight line, but the slopes of these best-fit lines are found to differ from each other and all differ from that of pure sand. For example, the M values for mixtures FS80G20 and FS60G40 are quantified to be 1.13 and 1.08, respectively, whereas the M values for FS80C20 and FS60C40 are 1.26 and 1.34, respectively. If using the CSL of pure sand as a reference, the addition of spherical glass beads into Fujian sand causes a clockwise rotation of the CSL in the q–p plane, meaning that the M value decreases. In contrast, adding crushed glass beads into Fujian sand causes an anti-clockwise rotation of the CSL, thus leading to an increase in the M value. The changes in M values are believed to be associated mainly with the differences in the particle shape of these materials.

In the CSSM framework, M corresponds to the critical state friction angle ϕ_{cs} – a key design parameter in geotechnical applications – as follows:

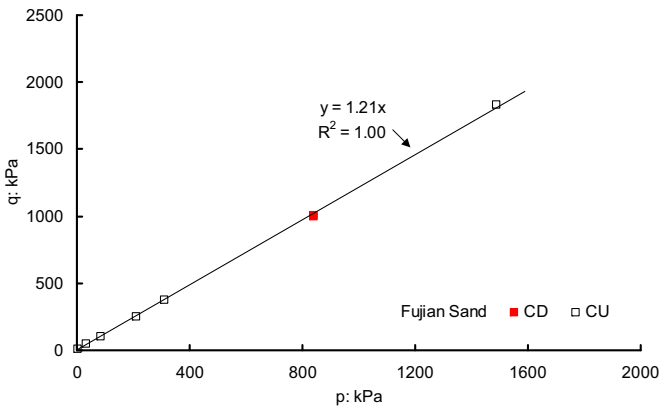

Fig. 10. Critical states of Fujian sand in q–p' plane from undrained and drained tests.

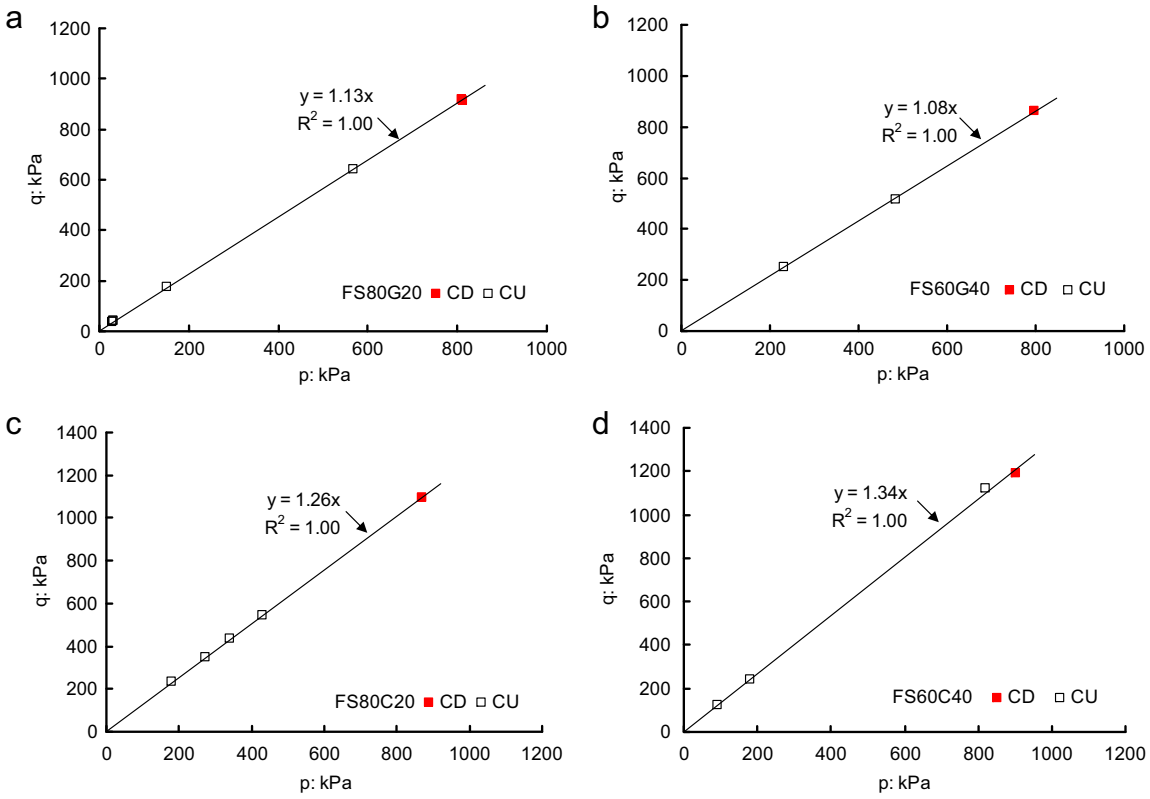

Fig. 11. Critical states of binary mixtures in q–p' plane: (a) FS80G20; (b) FS60G40; (c) FS80C20; (d) FS60C40.

$$\sin \phi_{cs} = \frac{3M}{6 + M} \tag{7}$$

Given an M value of 1.21 for Fujian sand, ϕ_{cs} is determined to be 30.3°, which is typical for uniform quartz sands reported in the literature. Of interest here is how ϕ_{cs} of Fujian sand varies with the percentage of the additives. The answer to this question is graphically presented in Fig. 12, which shows totally different effects of the additives: the effect can be a linear

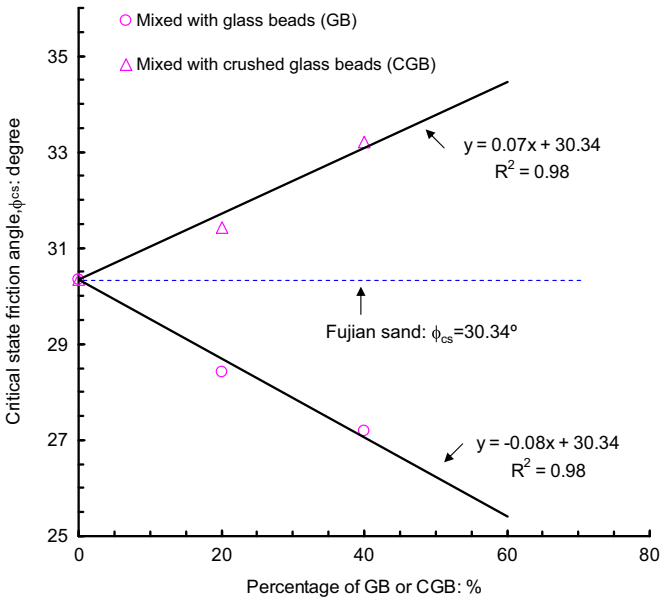

Fig. 12. Variation of critical state friction angle of binary mixtures.

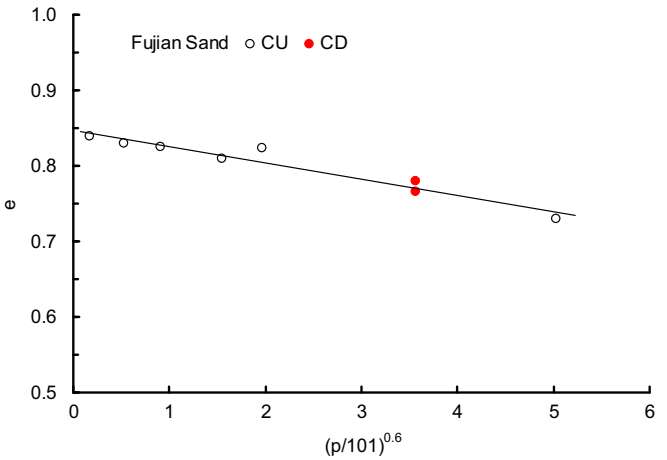

Fig. 13. Critical states of Fujian sand in e–p' plane in power-law form.

increase with the percentage of crushed glass beads or a linear decrease with the percentage of glass beads. The two trend lines in Fig. 12 are specified to share the same intercept that corresponds to ϕ_{cs} of Fujian sand, and one can see that the rate of variation of ϕ_{cs} for mixtures of Fujian sand and glass beads is slightly larger than that for mixtures of Fujian sand and crushed glass beads. The findings shown in Fig. 12 are in agreement with the experimental results on the effect of adding non-plastic fines to clean sands (Yang and Wei, 2012), but all materials in the current study are of sand size with uniform grading, rather than with a large size distribution as in the case of sand-fines mixtures.

4.2. Critical state locus in the e–p plane

The critical state data from both undrained and drained tests for Fujian sand are plotted in Fig. 13 using the power law in Eq. (4). A satisfactory representation of the critical state data with the power law is achieved as well for all mixtures, as

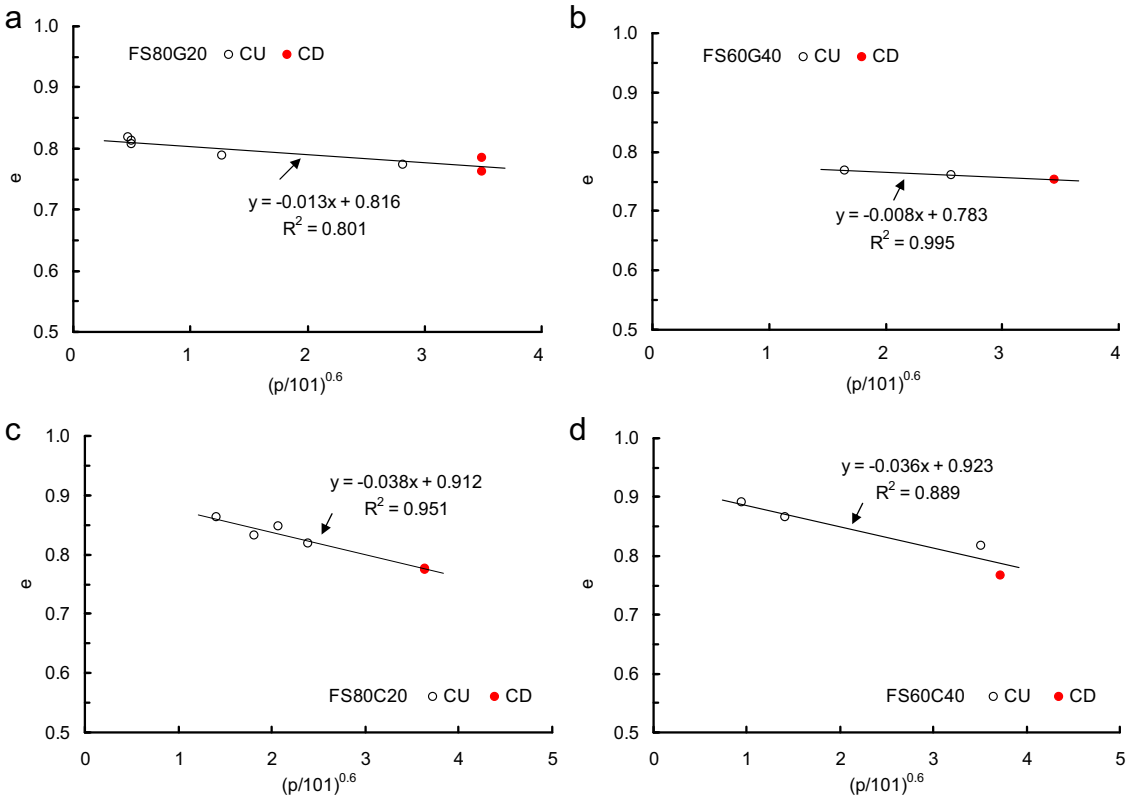

Fig. 14. Critical states of binary mixtures in e–p' plane: (a) FS80G20; (b) FS60G40; (c) FS80C20; (d) FS60C40.

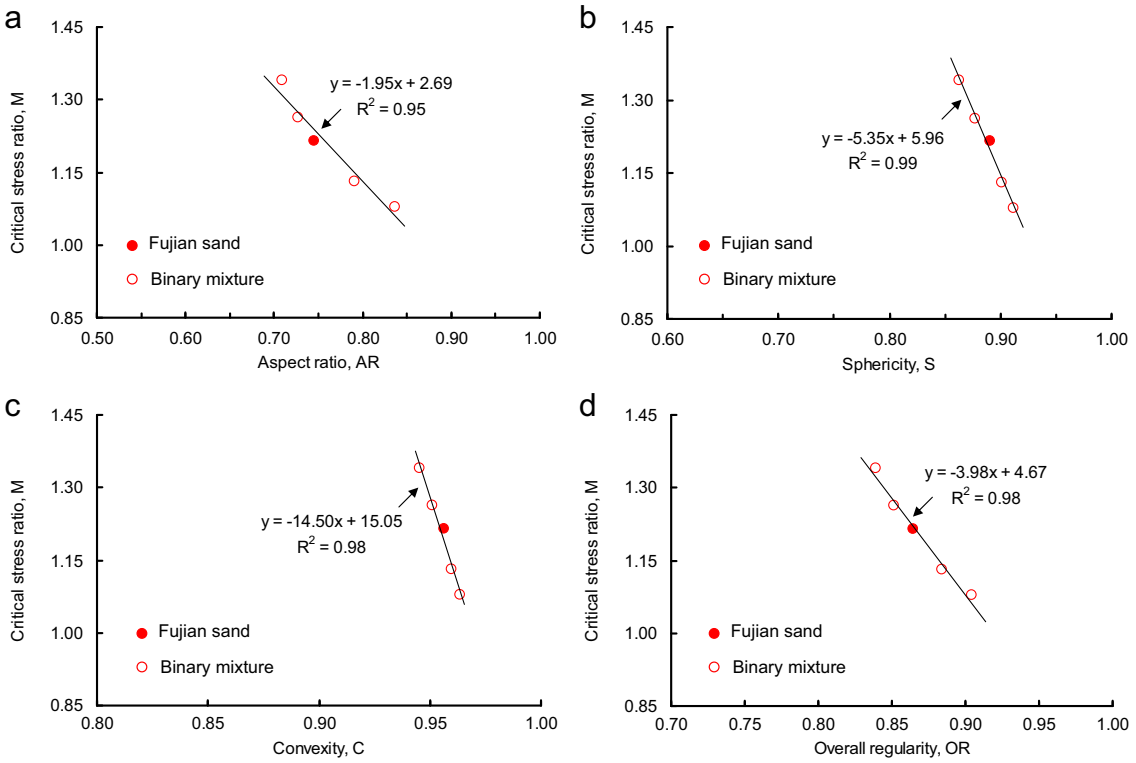

Fig. 15. Correlation of M with particle shape parameter: (a) aspect ratio; (b) sphericity; (c) convexity; (d) overall regularity.

shown in Fig. 14. A comparison of Figs. 13 and 14 indicates that the position of the CSL in the compression space varies and the variation appears to occur in both gradient and intercept. By using the CSL of Fujian sand as a reference line, it is found that when spherical glass beads were mixed with pure sand, the slope and intercept of the CSL tended to decrease, whereas when angular crushed glass beads were mixed with the sand the slope and intercept of the CSL tended to increase. The observed changes in the position of the CSL are thought to be mainly associated with varying particle shape, because all mixed and pure sand samples were controlled to have the same grading. In this connection, the mechanism for the observed changes is different from that for the movement of the CSL in the compression plane caused by adding fines into clean sand (e.g., Yang and Wei, 2012; Thevanayagam et al., 2002); for the latter case the mechanism is mainly associated with the significant change in particle size gradation.

Within the CSSM framework, the change in the position of the CSL implies that at a given effective confining stress and void ratio, granular materials with regular and rotund particles tend to be more susceptible to liquefaction than those with irregular and angular particles. This interpretation is well supported by the experimental results shown in Fig. 8 that the mixtures of pure sand and glass beads appear to be markedly more susceptible to liquefaction than the mixtures of the same sand with crushed glass beads. Due to limited space, other test results in support of this interpretation are not presented here.

5. Relating macro-scale and micro-scale properties

It has been found that as particle shape varies, the CSL may change its position in both the stress space and the compression space. Further attempt is now made to explore how the critical state parameters (M, ϕ_{cs}, e_Γ, λ_c) are related to the shape parameters (AR, S, C, OR). In Fig. 15a, the M values of the tested materials are plotted against their AR values. A strong correlation ($R^2=0.95$) is found between these two quantities, indicating that the M value decreases in an approximately linear manner with an increasing AR value. In other words, as the aspect ratio increases, the slope of the CSL in the q–p plane reduces. A similarly strong correlation is found between M and S (Fig. 15b) and between M and C (Fig. 15c), both showing an approximately linear reduction of the M value with increasing sphericity and convexity. Using the overall regularity (OR) as shape index, the dependence of M on particle shape can be characterized by

$$M = 4.67—3.98OR. \tag{8}$$

Given the relationship between M and ϕ_{cs}, the dependence of ϕ_{cs} on particle shape can be described as follows:

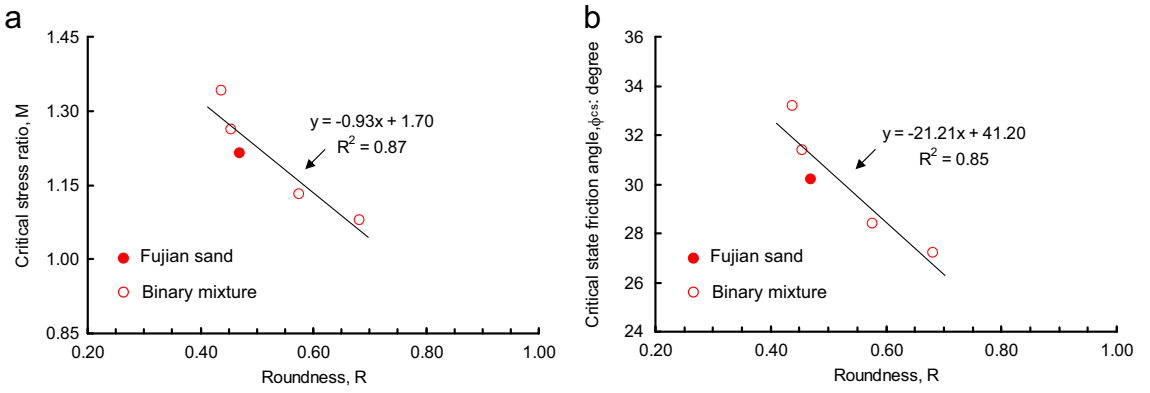

Fig. 16. Correlation of (a) M and (b) ϕ_{cs} with particle roundness.

$$\phi_{cs}(\text{deg}) = 109.03—90.9OR \tag{9}$$

The trend given by the above correlation is generally consistent with results from several previous studies on natural and crushed sands that ϕ_{cs} decreases with particle roundness (e.g., Cho et al., 2006; Rouse et al., 2008). Roundness describes the angularity of a particle and can be quantified as the ratio of the average radius of curvature of surface features to the radius of curvature of the maximum inscribed sphere (Wadell, 1932). To make a further comparison, the overall roundness of each of the test materials was quantified and the concept of combined roundness (Yang and Wei, 2012) was then used to calculate the roundness of mixtures (denoted as R; for ease of reference these values are included in Table 2).

The correlations of M and ϕ_{cs} with particle roundness are shown in Fig. 16a and b, respectively. Note that the correlation between ϕ_{cs} and R, given as

$$\phi_{cs}(\text{deg}) = 41.20–21.21R \tag{10}$$

has a coefficient of determination (0.85) that is comparable to the correlation developed by Cho et al. (2006):

$$\phi_{cs}(\text{deg}) = 42–17R \tag{11}$$

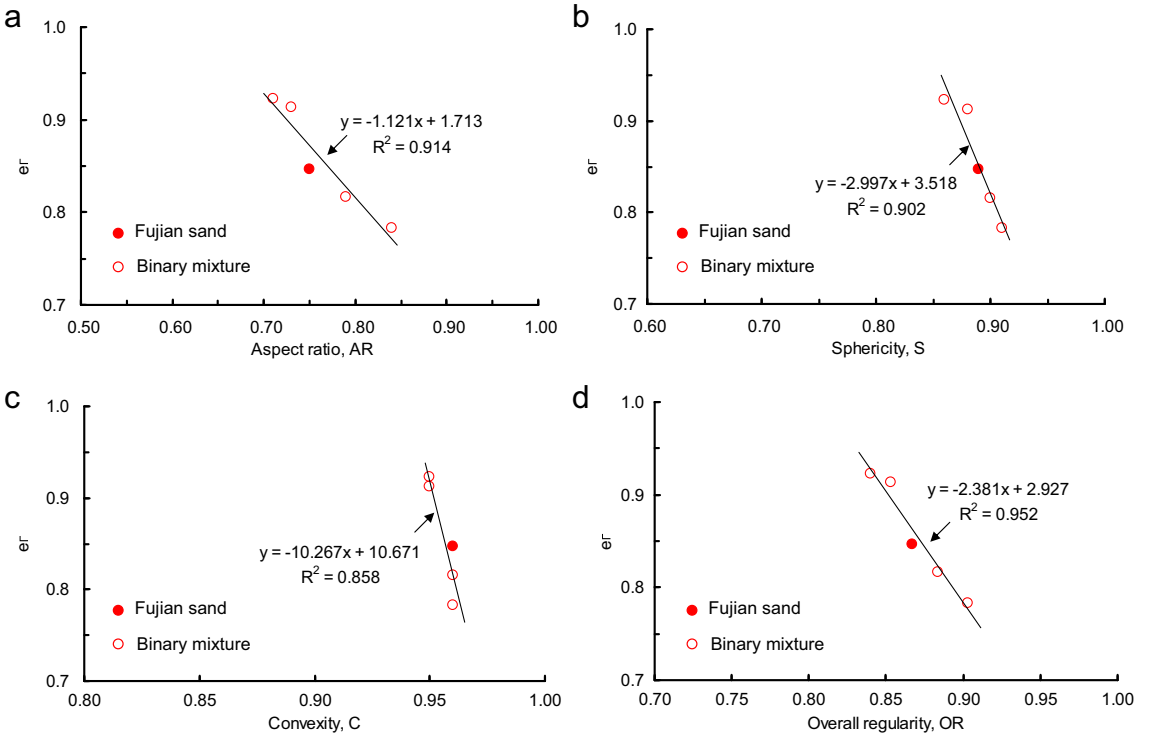

Fig. 17. Correlation of critical state parameter (e_r) with particle shape parameter: (a) aspect ratio; (b) sphericity; (c) convexity; (d) overall regularity.

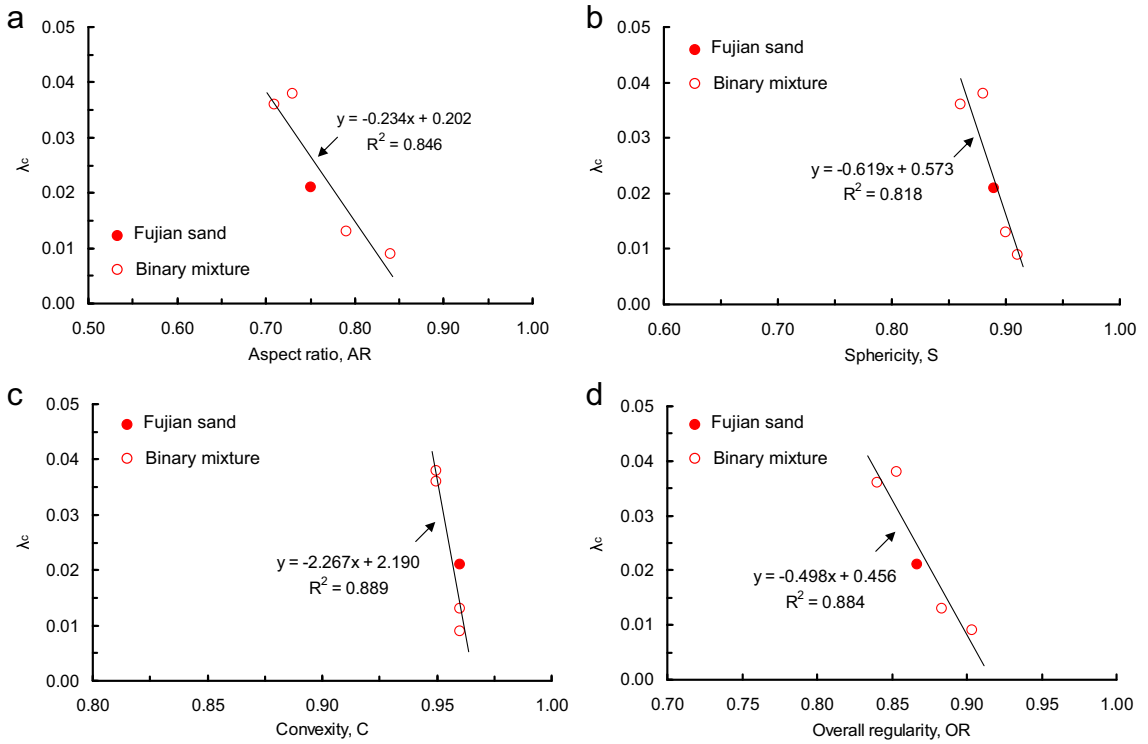

Fig. 18. Correlation of critical state parameter (λ_c) with particle shape parameter: (a) aspect ratio; (b) sphericity; (c) convexity; (d) overall regularity.

Compared with the correlations established for other shape parameters (*AR, S, C*, and *OR*), this coefficient is evidently lower. Another noteworthy point is the limiting case of roundness (i.e. $R=1$; approximately corresponding to spherical glass beads). For this case the correlation in Eq. (11) gives ϕ_{cs} a value of 25°, which is markedly higher than the measured value for uniform glass beads (~21°), reported by Cavarretta et al. (2010), whereas the correlation developed in this study gives a value (~20°) that is very close to the measured one.

The overall friction angle of a granular material may also be affected by surface roughness of the constituent particles which is quantified by the deviations in the direction of the normal vector of a real surface from its ideal form (Currence and Lovely, 1970) and is supposed to be linked with interparticle friction coefficient (μ_s). Several studies have examined the effect of μ_s on the shear behavior (e.g., Thornton, 2000; Dai et al., 2015) and the granular flow (da Cruz et al., 2005; Kamrin and Koval, 2014) by using the discrete element method (DEM). These simulations seem to suggest that the overall friction property is not sensitive to the interparticle friction coefficient if μ_s is above a threshold value (~0.27; corresponding to an interparticle friction angle of ~15°), whereas if μ_s is below this threshold the overall friction property tends to increase with μ_s. Cavarretta et al. (2010) made direct measurements of surface roughness of as-supplied and deliberately roughened glass beads and found that the difference in roughness caused no appreciable difference in uniaxial compression behavior. In the current study, the difference in surface roughness of the as-supplied and crushed glass beads is is presumably slight, and its influence on M and ϕ_{cs} is thus considered negligible as compared with the significant influence of particle shape and roundness.

The correlations between the intercept of the CSL (e_Γ) and the aspect ratio, sphericity and convexity are examined in Fig. 17. Apparently, e_Γ correlates to these shape parameters fairly well, giving a linear decrease of e_Γ with increasing aspect ratio, sphericity and convexity. Among the three shape measures, e_Γ appears to correlate best with aspect ratio. The shape effect on the intercept e_Γ can better be characterized by using overall regularity as follows:

$$e_r = 2.927 - 2.381OR \tag{12}$$

In Fig. 18, values of the gradient of the CSL (λ_c) for the tested materials are plotted against values of their shape parameters. A reasonably good correlation can be established between λ_c and each of the shape parameters, all suggesting that the slope of the CSL declines with increasing aspect ratio, sphericity and convexity. Similarly, the shape effect on λ_c can be quantified by use of overall regularity as.

$$\lambda_c = 0.456–0.498OR. \tag{13}$$

The above equation predicts that the slope of the CSL in the compression space tends to decrease as particle regularity

increases. Based on a compiled database for natural and crushed sands in the literature, Cho et al. (2006) reported no correlation between the slope of the CSL and particle shape. Two possible reasons might contribute to the failure to discover the relation: (a) Particle size gradation has an important influence on the position of the CSL but this influence was not isolated in their analysis (values of C_u in the database range from 1.2 to as high as 6.2); and (b) the CSL was represented by a straight line in the e-log$p$ plane but in many cases the CSL is a curved line on the semi-log form.

6. Implications for critical state theory

The relations expressed in Eqs. (8) and (9), and (12) and (13) give a consistent trend that the critical state parameters (M, ϕ_{cs}, e_Γ, λ_c) tend to decrease with increasing particle regularity. The observed dependence of ϕ_{cs} on particle shape implies that at the critical state when dilation is thought to vanish, the overall shearing resistance of granular material is mobilized not only by interparticle friction that is mainly dependent on particle mineralogy and surface roughness, but also by rearrangements of the particles. In this respect, regular and rotund particles with high OR values, when subjected to loading, are easier to move by rolling than irregular particles with low OR values, thereby giving rise to lower shearing resistance. In particular, for the limiting case that the material is composed of perfectly spherical particles (i.e. $OR=1$), the relationship in Eq. (9) predicts a considerably low value of ϕ_{cs} (18.1°). This value is comparable to the measured value for uniform glass beads (~21°), and the difference is considered to be associated mainly with the fact that manufactured glass beads are not perfect in sphericity but usually contain more or less defects in geometry (Yang and Gu, 2013). For example, for the glass beads used in this study, the overall regularity was determined to be 0.964 (Table 2), which is a little less than one. If this shape value is substituted into Eqs. (8) and (9), one obtains $\phi_{cs}=21.4°$ and $M=0.83$, which are strikingly close to the measured values for glass beads.

In the critical state theory, the intercept of the CSL in the volumetric compression space corresponds to an extreme void ratio for the material at an extremely low mean effective stress, and the gradient of the CSL corresponds to the compressibility of the material. In this respect, regular and rotund particles, because of the ability to move more efficiently than irregular and angular particles in loading, tend to form a denser packing state that would thus be less compressible. This explains the observed trend that e_Γ and λ_c tend to reduce with increasing overall regularity of particles (Figs. 17 and 18; Eqs. (12) and (13)). On the other hand, the finding that a granular material with irregular and angular particles is more compressible (i.e. larger λ_c) than its counterpart with regular and rotund particles has an important implication for liquefaction evaluation: that is, as compressibility increases the opportunity for the material to form a meta-stable structure during consolidation is reduced, so that it is unlikely for the material to undergo severe liquefaction. This hypothesis is supported by the experimental results shown in Fig. 8 that the nature of the response exhibited by mixtures with irregular particles is essentially dilative, either with a very limited loss of strength followed by strain hardening or without any strength loss.

While Eq. (13) gives a fairly good correlation between λ_c and particle overall regularity, a point remains that deserves further discussion. That is, when overall regularity goes towards the limiting case, for example $OR=1$ for perfectly spherical particles, the linear function gives a negative λ_c: physically this prediction does not make sense. To overcome this shortcoming, a power-law function rather than the linear function is used to best fit the data (Fig. 19), yielding the following relationship:

$$\lambda_c = 0.001(OR)^{-21.4}. \tag{14}$$

Compared with the linear relationship, the above equation not only provides a much improved correlation, with R^2 changing from 0.884 to 0.943, but also gives a sound prediction of λ_c for the limiting case: $\lambda_c=0.001$ for $OR=1$. The extremely low value of λ_c implies that the idealized spherical material is markedly less compressible in comparison with

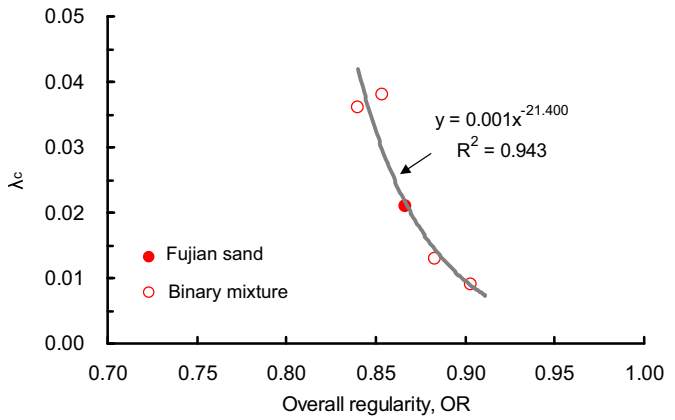

Fig. 19. Improved correlation between critical state parameter (λ_c) and overall regularity.

uniform quartz sands (e.g., λ_c=0.02 for Fujian sand).

The relationships expressed in Eqs. (8), (9), (12), and (14) are built upon experimental results on granular materials of uniform gradation. Many analytical, numerical and experimental studies on granular materials have focused on uniform size distribution, for example uniform quartz sands and glass beads in experiments (Verdugo and Ishihara, 1996; Goddard, 2014) and uniform or mono-size spheres in DEM simulations (Jenkins et al., 2005; Fleischmann et al., 2013). In this regard, an attractive value of these relationships is that they can be used as a first approximation to estimate critical state parameters of these uniform granular materials from their shape measures. Attempt made on uniform glass beads and Toyoura sand indeed gives reasonable predictions. As far as the influence of varying gradation is concerned, additional test results on Fujian sand of three different gradings (C_u=1.58, 2.22, 3.56) have found no appreciable difference in M (or ϕ_{cs}) values, meaning that the influence of gradation is insignificant on M; this finding is consistent with several DEM simulations in the literature. These tests also suggest that the slope of the CSL (λ_c) is not sensitive to changes in gradation, but the void ratio intercept e_Γ is more significantly affected in that it declines with increasing C_u. Given the scope of this paper, a detailed discussion of these test results is not presented here. Future work is also needed to further examine the influence.

Of final note is that the relationships developed in this study indicate a high sensitivity of the critical state parameters to the variation of particle shape. An apparently small variation in shape value may give rise to appreciable changes in the critical state parameters. For example, when *OR* changes from 0.82 to 0.86, ϕ_{cs} will reduce by 3.6°, from 34.5° to 30.9°, and the slope of the CSL reduces by over 60%, from 0.07 to 0.025. This sensitivity underlines the inadequacies of qualitative descriptions of particle shape in current practice and the need for accurate measurement of particle shape.

7. Summary and conclusions

This paper presents an experimental study exploring relationships between critical state properties and particle shape parameters for a fundamental understanding of the mechanics of granular materials. A sequence of binary mixtures with the same grading but different particle shape was produced for laboratory testing, so that the influence of size gradation was ruled out and the observed differences in macro-scale response were attributed primarily to the differences in particle shape. A robust laser scanning technique was used to make objective and accurate measurements of particle shape, and the concept of combined shape measure was proposed to describe the overall shape of binary mixtures. The main results and findings of the study are summarized as follows.

(a) A general trend has been established for all three shape measures (i.e. aspect ratio, *AR*; sphericity, *S*; and convexity, *C*) that as shape value increases, the particle tends to be more rotund. The new shape index, referred to as overall regularity (*OR*) and defined as the average of *AR*, *S* and *C*, can be used to give a collective description for the geometry of the particle. The higher the overall regularity the more regular and rotund the particle.

(b) Both undrained and drained tests provide solid evidence that varying particle shape can significantly alter the overall response and shearing resistance of granular soils. For a given initial state, in terms of the effective confining stress and void ratio, the liquefaction susceptibility of a granular soil was shown to be highly dependent on its particle shape. As particle regularity increases the soil tends to be more susceptible to liquefaction.

(c) With increasing particle regularity the critical state locus (CSL) in the stress space tends to rotate clockwise, whereas a decrease in particle regularity leads to an anti-clockwise rotation of the CSL. For either case the degree of rotation or the level of change in the gradient of the CSL (i.e. M value) is mainly associated with the level of change in particle shape.

(d) In the compression space an increase in particular regularity tends to reduce the intercept and the slope of the CSL, whereas a decrease in particular regularity tends to raise the intercept and the slope of the CSL. The changes in the position of the CSL imply that at a given effective confining stress, the void ratio required for liquefaction tends to decrease with increasing particle regularity or tends to increase with decreasing particle regularity.

(e) Quantitative relationships have been established between the critical state properties (M, ϕ_{cs}, e_Γ, λ_c) and the shape parameters (*AR, S, C, OR*), all suggesting that M, ϕ_{cs}, e_Γ, and λ_c decrease with increasing aspect ratio, sphericity, convexity and overall regularity. The critical state properties appear to be sensitive to the variation of shape parameters, underscoring the importance of accurate measurement of particle shape.

(f) The relationships allow the influence of particle shape on critical state properties to be evaluated quantitatively, thereby providing a way to construct CSSM-based macro-scale constitutive models with intrinsic micro-scale properties built in. Further experimental and numerical work towards refinement and improvement of these relationships is worthwhile.

Acknowledgments

The work was supported by the National Natural Science Foundation of China through the Overseas Young Investigator Award (No. 51428901) and by the Research Grants Council of Hong Kong through the Collaborative Research Fund (No. CityU8/CRF/13G). The various forms of support provided by the University of Hong Kong during the course of the research are highly acknowledged as well.

References

Alshibi, K.A., Druckrey, A.M., Al-Raoush, R.I., Weiskittel, T., Lavrik, N.V., 2014. Quantifying morphology of sands using 3D imaging 10.1061/(ASCE)MT.1943-5533.0001246..

Altuhafi., F., O'Sullivan., C., Cavarretta., I., 2013. Analysis of an image-based method to quantify the size and shape of sand particles. J. Geotech. Geoenviron. Eng. ASCE, 139; 1290–1307.

Anand, L., Gu, C., 2000. Granular materials: constitutive equations and strain localization. J. Mech. Phys. Solids 48, 1701–1733.

Andreotti, B., Forterre, Y., Pouliquen, O., 2013. Granular Media: Between Fluid and Solid. Cambridge University Press, Cambridge.

Been, K., Jefferies, M.G., 1985. A state parameter for sands. Géotechnique 35 (2), 99–102.

Bowman, E.T., Soga, K., Drummond, W., 2001. Particle shape characterization using Fourier descriptor analysis. Géotechnique 51 (6), 545–554.

Cavarretta, I., 2009. The influence of particle characteristics on the engineering behaviour of granular materials (Ph.D. thesis). Imperial College London.

Cavarretta, I., Coop, M., O'Sullivan, C., 2010. The influence of particle characteristics on the behaviour of coarse grained soils. Géotechnique 60 (6), 413–423.

Cho, G., Dodds, J., Santamarina, J.C., 2006. Particle shape effects on packing density, stiffness and strength: natural and crushed sands.. J. Geotech. Geoenviron. Eng. ASCE, 132; 591–602.

Collins, I., Houlsby, G., 1997. Application of thermomechanical principles to the modelling of geotechnical materials. Proc. R. Soc. Lond. A 453, 1975–2001.

Currence, H.D., Lovely, W.G., 1970. The analysis of soil surface roughness. Trans. ASAE 13, 710–714.

Dai, B.B., Yang, J., Zhou, C.Y., 2015. Observed effects of interparticle friction and particle size on shear behavior of granular materials. Int. J. Geomech., ASCE http://dx.doi.org/10.1061/(ASCE)GM.1943-5622.0000520.

da Cruz, F., Emam, S., Prochnow, Roux, J., Chevoir, F., 2005. Rheophysics of dense granular materials: Discrete simulation of plane shear flows. Phys. Rev. E 72, 021309.

Fleischmann, J.A., Drugan, W.J., Plesha, M.E., 2013. Direct micromechanics derivation and DEM confirmation of the elastic moduli of isotropic particulate materials. J. Mech. Phys. Solids 61, 1569–1584.

Fonseca, J., O'Sullivan, C., Coop, M.R., Lee, P.D., 2012. Non-invasive characterization of particle morphology of natural sands. Soils Founds 52 (4), 712–722.

Gajo, A., Bigoni, D., Wood, D.M., 2004. Multiple shear band development and related instabilities in granular materials. J. Mech. Phys. Solids 52, 2683–2724.

Gu, X.Q., Yang, J., 2013. A discrete element analysis of elastic properties of granular materials. Granul. Matter 15 (2), 139–147.

Goddard, J.D., 2014. Continuum modeling of granular media. Appl. Mech. Rev. 66, 050801.

Jaeger, H.M., Nagel, S.R., Behringer, R.P., 1996. Granular solids, liquids, and gases. Rev. Mod. Phys. 68, 1259–1273.

Jenkins, J., Johnson, D., Ragione, L., Makse, H., 2005. Fluctuations and the effective moduli of an isotropic, random aggregate of identical, frictionless spheres. J. Mech. Phys. Solids 53, 197–225.

Kamrin, K., Koval, G., 2014. Effect of particle surface friction on nonlocal constitutive behavior of flowing granular media. Comput. Part. Mech. 1, 169–176.

Krumbein, W.C., Sloss, L.L., 1963. Stratigraphy and Sedimentation, 2nd ed. Freeman, San Francisco.

Ladd, R.S., 1974. Specimen preparation method and liquefaction of sands.. J. Geotech. Eng. Div. ASCE, 100; 1180–1184.

Li, X.S., Dafalias, Y.F., 2015. Dissipation consistent fabric tensor definition from DEM to continuum for granular media. J. Mech. Phys. Solids 78, 141–153.

Li, X.S., Wang, Y., 1998. Linear representation of steady-state line for sand.. J. Geotech. Geoenviron. Eng. ASCE, 124; 215–1217.

McDowell, G.R., Bolton, M.D., Robertson, D., 1996. The fractal crushing of granular materials. J. Mech. Phys. Solids 44, 2079–2102.

Nedderman, R., 1992. Statics and Kinematics of Granular Materials. Cambridge University Press, Cambridge.

Nixon, S.A., Chandler, H.W., 1999. On the elasticity and plasticity of dilatant granular materials. J. Mech. Phys. Solids 47, 1397–1408.

Poulos, S.J., 1981. The steady state of deformation. J. Geotech. Eng. Div. ASCE, 107; 553–562.

Rothenburg, L., Kruyt, N.P., 2004. Critical state and evolution of coordination number in simulated granular materials. Int. J. Solids Structures 41, 5763–5774.

Rouse, P.C., Fannin, R.J., Shuttle, D.A., 2008. Influence of roundness on the void ratio and strength of uniform sand. Géotechnique 58 (3), 227–231.

Rudnicki, J.W., Rice, J.R., 1975. Conditions for the localization of deformation in pressure-sensitive and dilatant materials. J. Mech. Phys. Solids 23, 371–394.

Satake, M., Jenkins, J.T., 1988. Micromechanics of Granular Materials. Elsevier, Amsterdam.

Schofield, A.N., Wroth, C.P., 1968. Critical State Soil Mechanics. McGraw-Hill, London.

Spencer, A.J.M., 1964. A theory of the kinematics of ideal soils under plane strain conditions. J. Mech. Phys. Solids 12, 337–351.

Sukumaran, B., Ashmawy, A.K., 2001. Quantitative characterisation of the geometry of discrete particles. Géotechnique 51 (7), 19–27.

Sympatec, 2008. Windox-operating Instructions Release 5.4.1.0, Sypatec GmbH. Clausthal-Zellerfeld, Germany.

Taiebat, M., Dafalias, Y.F., 2008. SANISAND: simple anisotropic sand plasticity model. Int. J. Numer. Anal. Meth. Geomech. 32 (8), 915–948.

Thevanayagam, S., Shenthan, T., Mohan, S., Liang, J., 2002. Undrained fragility of clean sands, silty sands, and sandy silts. J. Geotech. Geoenviron. Eng. ASCE, 128; 849–859.

Thornton, C., 2000. Numerical simulations of deviatoric shear deformation of granular media. Géotechnique 47 (2), 319–329.

Verdugo, R., Ishihara, K., 1996. The steady state of sandy soils. Soils Founds 36 (2), 81–91.

Wadell, H., 1932. Volume, shape, and roundness of rock particles. J. Geol. 40 (5), 443–451.

Wichtmann, T., Triantafyllidis, T, 2009. Influence of the grain-size distribution curve of quartz sand on small strain shear modulus G_{max}.. J. Geotech. Geoenviron. Eng. ASCE, 135; 1404–1418.

Wood, D.M., 1990. Soil Behaviour and Critical State Soil Mechanics. Cambridge University Press, Cambridge.

Yang, J., Dai, B.B., 2011. Is the quasi-steady state a real material behaviour? A micromechanical perspective. Géotechnique 61 (2), 175–183.

Yang, J., Gu, X.Q., 2013. Shear stiffness of granular material: does it depend on particle size? Géotechnique 63 (2), 165–179.

Yang, J., Wei, L.M., 2012. Collapse of loose sand with the addition of fines: the role of particle shape. Géotechnique 62 (12), 1111–1125.